AR-005-706

NUMERICAL SIMULATION OF DETONATION TRANSFER BETWEEN GASEOUS EXPLOSIVE LAYERS

D.A. JONES, R. GUIRGUIS AND E. S. ORAN

MATERIALS RESEARCH LABORATORY
DSTO

NUMERICAL SIMULATION OF DETONATION TRANSFER BETWEEN GASEOUS EXPLOSIVE LAYERS

D.A. Jones, R. Guirguis*
and E.S. Oran†

MRL Research Report
MRL-RR-1-89

ABSTRACT

The development of a two-dimensional computer code to simulate detonation transfer between explosive layers is described. The code is based on previous models developed at the Laboratory for Computational Physics and Fluid Dynamics at Naval Research Laboratory, Washington, DC to study the structure of layered detonations and the details of detonation transmission from one medium to another. The code has been configured to simulate experiments conducted at the University of Michigan on the lateral transfer of detonation and shock phenomena between different gaseous layers. Preliminary calculations with the code show that the computations produce many of the structures seen in the Michigan experiments and also provide detailed descriptions of the detonation transmission and evolving structure.

* Science Applications International Corporation, McLean, Virginia, USA
† Naval Research Laboratory, Washington, DC, USA

Published by DSTO Materials Research Laboratory
Cordite Avenue, Maribyrnong, Victoria, 3032 Australia
Telephone: (03) 319 4499
Fax: (03) 318 4536

AR No. 005-706

AUTHORS

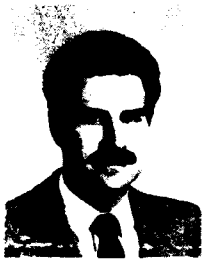

David Jones graduated from Monash University in 1972 with a BSc(Hons). He obtained his PhD from Monash in 1976. His thesis was titled "Anisotropic diffusion in the Townsend-Huxley experiment". After working at Strathclyde University, London University and the University of Sydney he joined MRL in 1983. He has worked on the numerical modelling of shaped charge warheads and slapper detonator devices. From February 1987 to May 1988 he was a Visiting Scientist at the Laboratory for Computational Physics and Fluid Dynamics at the Naval Research Laboratory in Washington DC. While there he worked on advanced computational fluid dynamics.

Dr Raafat H. Guirguis is employed by Science Applications International Corporation, McLean, Virginia.

Dr Elaine S. Oran works at the Naval Research Laboratory for Computational Physics and Fluid Dynamics, Washington, DC.

CONTENTS

		Page
1.	INTRODUCTION	7
2.	DESCRIPTION OF MODEL	8
3.	NUMERICAL SOLUTION	10
4.	CODE TESTING AND RESULTS	12
5.	DISCUSSION	14
6.	ACKNOWLEDGEMENTS	15
7.	REFERENCES	16

NUMERICAL SIMULATION OF DETONATION TRANSFER BETWEEN GASEOUS EXPLOSIVE LAYERS

1. INTRODUCTION

The transmission and reflection of shock and detonation waves through layered materials consisting of combinations of inert materials of different shock impedences, or combinations of inert and detonable materials, are of fundamental importance in many areas of military interest. Recent examples at MRL which consider shock transmission normal to the layers have included studies of shock propagation through copper/kapton/copper layers for the analysis of a shock compression conduction switch [1], and the transmission of impact shocks through metal/explosive layers for the analysis of the jet initiation of covered explosives [2]. When layered explosives are involved an interesting question is whether a suitable combination of explosives can enhance the effectiveness of the energy transmission compared to a pure explosive with the same total energy.

Interesting effects also occur when a detonation propagates along an explosive layer and then comes into contact with a bounding explosive. If the inner and bounding explosives are identical, the layered detonation pattern represents the diffraction that occurs when a detonation propagates past a step or an increase in cross-sectional area. With a suitable choice of symmetry axis this system can also represent the propagation of a detonation from a smaller into a larger tube, or an inner explosive sheathed in an outer explosive.

When solid explosives are used to study detonation transfer between layers it is very difficult to observe the complex interactions which develop. The problem is very much simpler for gaseous detonation transfer however, as pulsed laser Schlieren photography is an established method for studying complex structures in gaseous explosives. At the University of Michigan this technique has been combined with a specially designed shock tube to visualize transmitted shock and detonation structures in layered detonations for an extensive combination of explosives [3-6]. The experimental arrangement consists of two adjacent 1.6 cm x 1.6 cm square detonation tubes over three metres in length. A test section of length 15.2 cm or 19 cm is included and the different gases are initially separated by a nitrocellulose film of about 50 µm thickness. A stable detonation is initiated in the primary detonation tube and the interaction between the two mixtures begins when the detonation in the primary tube comes into contact with the film. In the initial phase of the interaction an explosive bubble or blast wave propagates into the secondary mixture. Further progress of the interaction then depends on the properties of both of the explosive mixtures.

In a series of experiments recently reported [5], the primary detonation tube contained a stoichiometric mixture of H_2 and O_2 while the secondary tube contained a variable mixture of H_2 and O_2. The exact composition of the explosive in the secondary tube is described by the equivalence ratio ϕ, which is defined to be the ratio of the amount of fuel to oxygen for the given system, divided by the same ratio for a stoichiometric system. In the experiments described in [3] the equivalence ratio of the mixture varied between 0.15 and 3.5. Three main modes of interaction were observed as the equivalence ratio of the bounding explosive was increased. In the first mode, ($\phi < 0.25$), only an oblique shock was induced in the mixture and there was no detonation. In the second mode ($0.35 < \phi < 1.0$) detonation was initiated directly, while in the third mode ($0.35 < \phi < 4.5$) detonation was initiated only after a Mach reflection of the induced oblique shock from the lower wall.

Shock polar analysis of the steady state interaction and the reflection from the lower wall have been used to analyse the different modes of interaction. A two-gamma method described by Liou [7] has been used to compute the oblique shock and detonation angles in the bounding explosive. The detonation angles computed using this method follow the trend of the experimental results, although the computed results are significantly below the measured values. Accurate analysis of the transient processes which occur as the explosive bubble first propagates into the bounding explosive cannot be treated using this approach however and require detailed numerical simulation.

The purpose of this report is to describe the development of a two-species reactive hydrocode to model these transient processes. The code described here is based on the Reactive Shock Models described by Oran and Boris [8]. The convective transport equations are solved using the Flux-Corrected Transport (FCT) algorithm developed in the Laboratory for Computational Physics and Fluid Dynamics at the Naval Research Laboratory [9,10,11]. The particular FCT algorithm used has fourth-order accuracy and can reproduce discontinuities with small dispersion errors and minimal numerical diffusion. It has already been used successfully to study Mach reflection of detonation waves in a variety of simulations [12,13].

As the basic reactive shock model used in this work has been fairly extensively described elsewhere [12,14] our description of the two-species model (Section 2), and its numerical implementation (Section 3), is relatively brief and concentrates mainly on those aspects unique to the geometry and two-species nature of the problem. A detailed discussion of the testing at each stage of code development and a comparison of the numerical simulations with the experimental results is presented in Section 4.

2. DESCRIPTION OF MODEL

The code developed here is based on similar models described recently by Guirguis et al. [12]. The Euler equations for compressible flow are solved assuming perfectly rigid and smooth walls. Two-dimensional rectangular geometry is employed with uniform grid spacing and fixed cell sizes in the x and y directions. The complexity and extent of the interactions behind the leading shock front make the use of moving or adaptive gridding techniques [8] inappropriate for this particular problem.

The equations for the conservation of mass, momentum and energy are

$$\frac{\partial \rho}{\partial t} + \nabla \cdot (\rho \mathbf{V}) = 0 \qquad (1)$$

$$\frac{\partial(\rho u)}{\partial t} + \nabla \cdot (\rho u \mathbf{V}) = -\frac{\partial P}{\partial x} \tag{2a}$$

$$\frac{\partial(\rho v)}{\partial t} + \nabla \cdot (\rho v \mathbf{V}) = -\frac{\partial P}{\partial y} \tag{2b}$$

$$\frac{\partial E}{\partial t} + \nabla \cdot (E\mathbf{V}) = -\nabla \cdot (P\mathbf{V}). \tag{3}$$

Here ρ is the density, u and v the x and y components of the velocity vector **V**, P is the scalar pressure, and E is the total energy per unit volume, defined by

$$E = \rho e + \frac{1}{2}\rho(u^2 + v^2), \tag{4}$$

where e is the specific internal energy.

Equations (1) through (3) are solved using the JPBFCT algorithm (a version of ETBFCT, documented in [15]) and operator splitting in the x and y directions. The rigid barrier separating the two detonation tubes runs along the x direction and is included in the calculation during the y integration. Depending on whether the x-coordinate is before or after the end of the barrier, the y integration is split into either two or one loops, with the end points of the loops being the upper and lower boundaries of each tube separately, or the upper and lower boundaries of the combined tube (see Figure 1).

The total density ρ is the sum of the densities of species one and two

$$\rho = \rho_{SP1} + \rho_{SP2}. \tag{5}$$

Each species is convected separately with the fluid velocity and normalised after each time step. The species are initially separated in the upper and lower detonation tubes but are allowed to mix freely as the detonation in the upper tube encounters the end of the dividing barrier.

A perfect-gas equation of state is used for each species, ie. $P_i = \rho_i R_i T$, where R_i is the specific gas constant for species i, and T is the equilibrium temperature of both species. In all of the calculations described below, the full details of the chemical reactions are not included in the model. Instead we use an induction parameter model that reproduces the essential features of the chemical reaction and energy release process. In this model, the chemical induction time and energy release rate are tabulated as a function of temperature, pressure, and stoichiometry. These have been obtained by integrating the full set of elementary chemical reactions for the hydrogen-oxygen-argon system using the CHEMEQ integration code [16]. Then a quantity called the induction parameter is defined and convected with the fluid in a Lagrangian manner. This parameter records the temperature history of a fluid element and, when the element has been heated for long enough, energy release is initiated. This model for including the properties of a chemical reaction mechanism in a numerical simulation was described originally by Oran et al. [20], and has been developed further by Kailasanath et al. [21] and Guirguis et al. [12].

The induction time τ^o, defined to be the time during which no energy is released, is fitted to an expression of the form

$$\tau^{o}(T,P) = A_{\tau}(P_{o}/P)\exp(E_{\tau}/RT) \tag{6}$$

In the second step, reactants are converted to products according to the finite reaction rate

$$d\omega/dt = -\omega A_{r}\exp(-E_{r}/R\,T), \tag{7}$$

where ω is the explosive mass fraction for species one or two. The constants A_{τ}, E_{τ}, A_{r} and E_{r} are calculated from the results of integrating the full set of chemical reactions for the system [16]. If f denotes the fraction of induction time elapsed at time t, then

$$\frac{df}{dt} = \frac{1}{\tau^{o}(T,P)}, \tag{8}$$

where f(0) = 0. However, as explained in [10], equation (8) is rewritten as

$$\frac{d(f\omega)}{dt} = \frac{\omega}{\tau^{o}}. \tag{9}$$

The final temperature and pressure within a cell are given by

$$T = \frac{e - \eta_1\omega_1\Delta E_1 - \eta_2\omega_2\Delta E_2}{\eta_1 Cv_1 + \eta_2 Cv_2} \tag{10}$$

$$P = \left(\frac{\eta_1}{mw_1} + \frac{\eta_2}{mw_2}\right) R^{*}\rho T \tag{11}$$

where η_i is the fraction of species i within the cell, and ΔE_i, Cv_i and mw_i are the energy release, specific heat and molecular weight for species i.

3. NUMERICAL SOLUTION

In a moving system, the time derivatives appearing in equations (6) and (9) denote a substantial derivative following the flow of the system. When combined with the continuity equation, they can be rewritten in the same form as equations (1) to (3), i.e.

$$\frac{\partial(\rho\omega_i)}{\partial t} + \frac{\partial(\rho\omega_i u)}{\partial x} + \frac{\partial(\rho\omega_i v)}{\partial y} = -\rho\omega_i A_{ri} e^{-E_{ri}/RT} \tag{12}$$

$$\frac{\partial(\rho\omega_i f_i)}{\partial t} + \frac{\partial(\rho\omega_i f_i u)}{\partial x} + \frac{\partial(\rho\omega_i f_i v)}{\partial y} = \frac{\rho_i\omega_i}{\tau^{o}_{i}} \tag{13}$$

for each species i. The solution procedure is then as follows: the variables ρ, ρu, ρv, E, $\rho\eta_i$, $\rho\omega_i$ and $\rho\omega_i f_i$ are advanced over the time step δt using the JPBFCT algorithm and operator splitting.[1] The specific internal energy is then calculated, the η_i renormalised, and the explosive mass fraction ω_i is then limited to a value less than or equal to one using

$$\omega_i = \min \{1.0, \omega_i\} \tag{14}$$

The fraction $\omega_i f_i$ is also limited according to

$$\omega_i f_i = \min \{\omega_i \eta_i, \omega_i f_i\} \tag{15}$$

The temperature and pressure are then calculated from equations (10) and (11).

Next, a burn subroutine is called to calculate the energy release if the induction time has elapsed. First Δt, the time remaining before the end of the induction period, is calculated and then compared with the hydrodynamic time step δt. There are two possibilities, Δt is either greater or less than δt. In the former case the fraction of induction time elapsed is advanced using an explicit solution to the equation

$$\frac{\partial(\rho\omega_i f_i)}{\partial t} = \rho_i \omega_i / \tau_i^o \tag{16}$$

and control returns to the main program. In the latter case the reaction variable ω_i is updated using an implicit solution to the equation

$$\frac{\partial(\rho\omega_i)}{\partial t} = - \rho\omega_i A_{ri} e^{-E_{ri}/RT}, \tag{17}$$

and a new temperature and pressure are calculated using equations (10) and (11).

The hydrodynamic time step δt is calculated using the Courant condition,

$$\delta t = CRNT * \min \left(\frac{\Delta \ell}{|vel| + c}\right), \tag{18}$$

where $\Delta \ell$ is the cell length in either the x or y direction, vel is the x or y component of velocity in each cell, and c is the sound speed. In a cell with a mixture of species one and two, the sound speed is calculated for each species separately and the greater of the two is used. In all the calculations to be described here, CRNT has the value 0.25.

A typical computational grid has 500 cells in the x direction and 80 cells in the y direction, with detonation initiated at the left hand boundary of the grid (x = 0). The value of the detonation velocity is such that it will typically take 3,000 to 4,000 cycles for the detonation to reach the right boundary. With a fixed right boundary, this means that in the initial stages of the calculation, a great deal of computational time is wasted computing properties of large areas of the grid in which nothing is happening. This is very time consuming and hence expensive. To solve this problem we decided to make the right

boundary movable. The number of cells in the x direction, NCX, is initially set to some conveniently small value, say NCX = 50, and then a check is made at the end of each time step to locate the right-most position of the leading shock. NCX is then adjusted to make sure that it is always five cells ahead of the position of the shock.

In each of the calculations described in the next section, the detonation in the primary tube was initiated by depositing an excess amount of energy into the first ten columns of the grid, thereby creating a blast wave that evolved into a detonation. The amount of energy per cell required to initiate detonation in the 2D code once the blast had progressed beyond the end of the barrier was typically an order of magnitude greater than that needed to initiate a stable CJ detonation in a one-dimensional code. This means that the detonation was considerably overdriven as it reached the end of the dividing barrier, a situation which did not apply in the actual experiments. Nevertheless, once the detonation passed the end of the barrier, its velocity rapidly approached the CJ value and some distance from the divider the pressure contours show patterns similar to those observed experimentally. Future use of the code however will include an option to input steady profiles for a stable CJ detonation taken from a one-dimensional code.

4. CODE TESTING AND RESULTS

Most of the experimental work at the University of Michigan reported to date has used mixtures of H_2 and O_2 in both the primary and secondary detonation tubes. As we do not yet have analytical expressions for induction times and energy release times for $H_2 - O_2$ mixtures with given equivalence ratio ϕ, the results described here use parameters for stoichiometric $H_2 - O_2$ diluted with Ar (H_2:O_2:Ar in ratio 2:1:7) which were available from previous simulations of shock tube experiments [17]. Values for each of the parameters defined in sections two and three for this mixture can be found in Table 1. A one-dimensional version of the code was used to calculate the CJ detonation velocity by depositing a small amount of excess energy into the system and allowing the simulation to run until the detonation velocity had reached a steady state. The value found using this method was 1600 m/sec.

The two-dimensional code was developed in several stages and tested at the completion of each stage. We began with a two-dimensional non-reactive hydrocode in rectangular geometry. The capabilities of the code at this stage are illustrated in Figure 2, which shows pressure contours every 400 cycles after an excess amount of energy was deposited into a few cells centered near the left boundary. Each of the surfaces is a rigid reflecting barrier. These figures clearly show the ability of the operator-split FCT code to model complex shock structures. Mach reflection of the blast wave from the top and bottom boundaries is clearly visible, and the convergent motion of the triple points can also be seen. The interaction of the shocks reflected from the left upper and lower corners with the converging triple points has produced quite a complicated shock structure after 1400 cycles. This structure progressively collapses onto itself and eventually results in the formation of a decaying plane wave moving to the right. The contour at 2600 cycles shows the shock structure just before this stage is reached.

Our first modification was to simulate a rigid barrier dividing the left half of the grid into separate upper and lower detonation tubes. Figure 3 shows a sequence of pressure contours in a calculation in which a blast wave was initiated in the upper tube and allowed to progress past the end of the barrier (which extends along half the length of the grid). The contour plot at 500 cycles shows the blast wave completely confined within the upper tube. The complex shock structure at this stage is very similar to the structure shown in Figure 2 after 1000 cycles. After 2500 cycles the structure has decayed to a

planar shock which has progressed past the end of the barrier and initiated a blast wave in the second tube. By 3500 cycles the shock is just about to reflect from the bottom of the second tube. The progression of the shock backwards into the second tube can also be seen.

The next stage was to make the code reactive by including a model that allows a single species to react, as decribed in the previous sections. At this stage we also set the number of cells in the x and y directions to 500 and 80 respectively, with $\Delta x = \Delta y = 4.0 \times 10^{-4}$ m. The value of the cell size was decided from previous work on this system. Figure 4 shows the result of initiating a detonation in the upper chamber by depositing an excess amount of energy into the first 10 columns of the grid. As the code at this stage is a single species code, the simulations represent experiments performed with the same reactive mixture in both the upper and lower tubes. For experiments with very thin films seperating the two similar layers, detonation is initiated almost instantaneously in the lower tube and Mach reflection of the detonation always occurs at the lower surface. When the film is thicker, a blast wave is transmitted and then the secondary detonation is initiated behind the Mach reflection from the lower wall. Examination of the pressure contours in Figure 4 shows similar behaviour to the experimental results found when very thin films are used, detonation is initiated directly by the blast wave and then a Mach reflection is formed on the lower boundary. The reflected wave patterns coincide nicely with the experimental results shown in [5].

The last stage involved converting the program into a two-species code. We did this by first defining new arrays and data for a second species and convecting the variables as outlined in the previous section. We then ran a calculation in which the second species was treated as an inert gas. Figure 5 shows pressure contours up to 3000 cycles for the case where species one is H_2:O_2:Ar in the ratio 2:1:7. The second species is the same mixture as the first, but it is constrained so that there is no energy release. The contrast with the results shown in Figure 4 is quite interesting, the inability of the second species to release energy has delayed the formation of the Mach stem and resulted in the formation of a complex reflected shock pattern which moves steadily through the system.

Finally, we further modified the code to allow the second species to detonate and ran a simulation with the same species in both tubes as a test of the program. Pressure contours up to 2000 cycles for this run are shown in Figure 6. These results should be compared with Figure 4, which used the same mixture in the upper and lower chambers but were generated using the single-species code. The results are very similar to one another but not quite identical. This could be due to slight differences in the initial condition between the two calculations, or to diffusional effects between the species across the interface.

Having fully developed the code and checked that it was giving satisfactory results, we then ran a simulation with different reactive species in the upper and lower chambers. Rather than spending a considerable amount of time calculating induction times and energy release times for the pure H_2–O_2 mixtures used in the experiments, we decided to retain the existing parameters for H_2:O_2:Ar and to vary those parameters in the same direction as the changes in the corresponding parameters for H_2–O_2 as ϕ varied from 0.125 to 2.5. We ran the chemical kinetics code CHEMOD [8] for selected values of initial pressure and temperature for H_2–O_2 mixtures with different values of ϕ. Over the range 0.125 to 1.0, we found that the induction time remained almost constant, while between 1.0 and 2.5, it more than doubled. The energy release time decreased only slightly over the full range. With stoichiometric H_2–O_2 in the upper chamber and a variable mixture of H_2 and O_2 in the lower chamber, the experiments show a change in interaction mode occurring around $\phi = 0.25$. Consequently we decided to change the parameter values for our model system to simulate a $\phi = 0.25$ mixture in the lower chamber. As we had found that there were only small changes in both induction time and energy release time between $\phi = 1.0$ and $\phi = 0.25$, we decided to leave these, and the value for γ, unchanged. We simulated the $\phi = 0.25$ mixture by setting $\Delta E_2 = 0.070$ kcal and

$mw_2 = 60.0$. In doing this we hoped to find Interaction Mode 1 type behaviour, ie., the secondary mixture is not initiated and only oblique shocks reflecting regularly from the lower wall are observed. The pressure contours for this calculation are shown in Figure 7. Direct initiation of the bounding explosive by the blast wave is again observed, but the reflection of this detonation from the lower boundary is quite different. The detonation in the bounding explosive initiated by the blast wave appears to be unstable and is rapidly quenched. The detonation is then re-initiated behind the shock reflected from the lower wall and a complicated pattern of an oblique shock connected to an oblique detonation appears to develop. This behaviour has been seen experimentally [18] and would be an interesting case for further study.

We next attempted to find Mode 1 behaviour by making further changes to the parameters specifying species two so that we simulated an even leaner mixture, ie., ϕ less than 0.25, but here we ran into problems. While the values for ΔE_2 and mw_2 chosen for ϕ = 0.25 lead to a stable detonation in a 1D code with a CJ velocity of approximately 1000 m/s, no detonation in a 1D code could be found when the parameter changes were made in the direction of decreasing ϕ. It appears that we have run into the detonation limit for our model system. Remembering that the original system is already quite dilute, this behaviour does not seem unreasonable. At this stage it was decided that further numerical simulation of the experimental results required expressions for the induction time and energy release time for pure H_2–O_2 mixtures. Calculation of these quantities is currently in progress, and results will be reported at a later date.

5. DISCUSSION

The results described in the previous section are particularly encouraging. When the materials in both tubes are identical the simulations show that a detonation is initiated directly in the second tube and a Mach reflection occurs at the lower boundary. When a leaner mixture is used in the second tube the simulations again show structures very similar to those seen in experiments. We cannot expect quantitative agreement between the simulations and experiments at this stage as the experiments were performed for mixtures of H_2 and O_2, while the simulations were performed for mixtures of H_2 and O_2 diluted with Argon. These diluted mixtures will have a lower detonation velocity as well as a more curved detonation front due to a longer induction time. Quantitative comparisons could be made if suitable constants could be determined for the induction model and energy release rate expression described in Section 2. These can be found by integrating a detailed chemical kinetics model [16], and checked by comparison with experimental values for induction times in undiluted H_2–O_2 mixtures [7]. Work along these lines is proceeding, and we anticipate that quantitative comparisons between the simulations and the experiments will be available at a future date.

Before further calculations are made with the code some minor changes could be made which would facilitate comparison of the output with the experimental results. Future runs should output contour plots of density, temperature, velocity, and reaction progress variables as well as pressure contours, as these would aid the interpretation of the complex shock and detonation structures. The experimental results are produced by Schlieren photography and this technique is sensitive to density gradients, whereas the results presented so far have only shown pressure contours. Density contours would provide a better comparison with experiment, and also enable important features such as contact surfaces to be seen. The experimental apparatus also has pressure transducers mounted on the top and bottom of the detonation tube so that pressure-time histories at selected positions can be obtained. This information could easily be output from the code so that further comparison with experiment could be made.

An important change which should be made involves the method of initiation. Currently the code is started by depositing excess energy into the first 10 cells in each row of the primary chamber. This creates a blast wave which almost instantaneously becomes an overdriven detonation which travels down the chamber. As the detonation reaches the end of the dividing barrier it is still highly overdriven, in contrast to the experiment, but soon decays to a stable detonation propagating at the CJ velocity. A much better method of initiation, one which parallels the experimental method much more closely, is to use output from a 1D reactive hydrocode as the input to the 2D code. A 1D reactive hydrocode was written during the course of this work to check the CJ values for the diluted H_2-O_2 mixtures used [19]. This code is also initiated by putting excess energy into the first few cells, but is then allowed to run for a sufficient amount of time so that a constant detonation velocity is established. At this stage variable profiles could be saved and used as input to the 2D code, which would ensure that a stable CJ detonation was approaching the end of the dividing barrier in the 2D simulation. This approach would also save computing time. Future work with the code will include this modification.

The code is currently configured to model the experiments conducted at the University of Michigan, but could easily be altered to simulate a wide variety of shock and detonation phenomena. The basic FCT subroutine used can treat rectangular, cylindrical, or spherical one-dimensional systems. The operator-splitting method used here for the two-dimensional simulation could also easily be extended to three dimensions. It is hoped that replacement of the perfect-gas equation-of-state (EOS) with a more general EOS will allow simulation of detonation in condensed explosives. This approach has already been used by Guirguis, Oran and Kailasanath, who used the HOM EOS [22] and an FCT algorithm to study the cellular structure of liquid nitromethane [12, 13]. FCT codes are also currently being developed at MRL to model shock propagation in metals, and preliminary results are encouraging [23].

All the calculations reported here were performed on the NRL Cray X-MP/12 computer. The code requires approximately 900,000 words of memory, and typical run times for 3,000 cycles were around 30 minutes.

6. ACKNOWLEDGEMENTS

This work was conducted while D.A. Jones was a Visiting Scientist at the Laboratory for Computational Physics and Fluid Dynamics at Naval Research Laboratory, Washington, DC, under a DSTO sponsored Scientific and Technical Update scheme. He wishes to thank Dr Jay P. Boris, Chief Scientist and Director of LCP & FD, for the opportunity to work in such a stimulating environment, and for the provision of excellent computing and support facilities. As this work was nearing completion we benefited greatly from lengthy discussions with Professor Martin Sichel. D.A. Jones also wishes tc thank Dr David Book for advice on aspects of FCT, and Drs Gopal Patnaik and Ken Laskey for help with programming problems.

7. REFERENCES

1. Richardson, D.D. MRL private communication
   Richardson, D.D. and Jones, D.A. (1986). A fast, low resistance switch for small slapper detonators (MRL Report MRL-R-1030). Maribyrnong, Vic.: Materials Research Laboratory.

2. Chick, M., Bussell, T.J., Frey, R.B. and Bines, A. Jet initiation mechanisms and sensitivities of covered explosives. Preprints of the Ninth Symposium (International) on Detonation, August 1989, Portland, Oregon.

3. Sichel, M., Liou, J.J., Kauffman, C.W. and Tovey, J.L. (1984). The interaction phenomena between adjacent detonating layers. Presented at the meeting of the Eastern Section of the Combustion Institute, November.

4. Liu, J.C., Liou, J.J., Sichel, M. and Kauffman, C.W. (1985). Diffraction by transmission of a detonation into a bounding explosive layer. Presented at the meeting of the Eastern Section of the Combustion Institute, November.

5. Liu, J.C., Liou, J.J., Sichel, M., Kauffman, C.W. and Nicholls, J.A. (1986). Diffraction and transmission of a detonation into a bounding explosive layer. Twenty-First International Symposium on Combustion.

6. Liu, J.C., Kauffman, C.W. and Sichel, M. (1987). The lateral interaction of detonating and detonable gaseous mixtures. International Conference on Detonation and Energetics of Reactive Systems, Warsaw, August 1987.

7. Liou, J.J. (1986). Analysis of the wave interaction between a propagating gaseous detonation and a bounding explosive layer. Ph.D. Thesis, University of Michigan.

8. Oran, E.S. and Boris, J.B. (1987). Numerical simulation of reactive flow. Elsevier Science Publishing Company.

9. Boris, J.P. and Book, D.L. (1973). Flux-corrected transport I : SHASTA, a fluid transport algorithm that works. Journal of Computational Physics, **11**, 32-69.

10. Book, D.L., Boris, J.P. and Hain, K. (1975). Flux-corrected transport II : generalizations of the method. Journal of Computational Physics, **18**, 248-283.

11. Boris, J.P. and Book, D.L. (1976). Flux-corrected transport III : minimal-error FCT algorithms. Journal of Computational Physics, **20**, 397-431.

12. Guirguis, R., Oran, E.S. and Kailasanath, K. (1986). Numerical simulations of the cellular structure of detonations in liquid nitromethane - regularity of the cell structure. Combustion and Flame, **65**, 339-365.

13. Guirguis, R., Oran, E.S. and Kailasanath, K. (1986). The effect of energy release on the regularity of detonation cells in liquid nitromethane. Twenty-first Symposium (International) on Combustion, The Combustion Institute, pp. 1659-1668.

14. Guirguis, R. and Oran, E.S. (1983). Reactive shock phenomena in condensed materials : formulation of the problem and method of solution (NRL Memo Report 5228). Washington, USA: Naval Research Laboratory.

15. Boris, J.P. (1976). Flux-corrected transport modules for solving generalized continuity equations (NRL Memo Report 3237). Washington, USA: Naval Research Laboratory.

16. Young, Jr., T.R. (1980). CHEMEQ - A subroutine for solving stiff ordinary differential equations (NRL Memo Report 4091). Washington, USA: Naval Research Laboratory.

17. Oran, E.S. and Boris, J.P. (1982). Weak and strong ignition. II. sensitivity of the hydrogen-oxygen system. Combustion and Flame, **48**, 149-161.

18. Professor Martin Sichel, personal communication, September 1988.

19. Jones, D.A., Guirguis, R. and Oran, E.S. A one-dimensional flux corrected transport code for detonation calculations, MRL Report in preparation.

20. Oran, E., Boris, J.P., Young, T.R. and Picone, J.M. (1981). Numerical simulations of detonations in hydrogen-air and methane-air mixtures. Proceedings of the 18th Symposium (International) on Combustion. Pittsburgh, PA: The Combustion Institute, 1641-1649.

21. Kailasanath, K., Oran, E.S. and Boris, J.P. (1985). Determination of detonation cell size and the role of transverse waves in two-dimensional detonations. Combustion and Flame, **61**, 199-209.

22. Mader, C.L. (1979). Numerical modelling of detonation. University of California Press, Los Alamos Series in Basic and Applied Sciences.

23. Tyndall, M.B. Numerical modelling of shocks in gases and metals. MRL Report in preparation.

SYMBOLS

ϕ	Equivalence ratio, i.e. fuel to oxygen ratio for a given system, divided by the same ratio for a stoichiometric system.
ρ	total mass density
ρ_i	mass density for species i
V	velocity vector
u, v	x and y components of velocity vector
P	pressure
E	total energy per unit volume
e	specific internal energy
ω_i	reaction variable for species i. $\omega = 1$ represents pure reactants, $\omega = 0$ represents pure products.
A_{ri}	frequency factor for species i in reaction rate expression
E_{ri}	activation energy for species i in reaction rate expression
τ_i	induction time for species i
$A_{\tau i}$	frequency factor for species i in induction time expression
$E_{\tau i}$	activation energy for species i in induction time expression
f_i	fraction of induction time elapsed for species i
η_i	fraction of species i within a cell
Cv_i	specific heat at constant volume for species i
mw_i	molecular weight of species i
ΔE_i	energy release for species i
C_i	sound speed of species i
δt	hydrodynamic time step
Δt	time remaining before end of induction period
R^*	universal gas constant

Table 1

Parameter Values for H_2:O_2:Ar in ratio 2:1:7

ΔE	=	0.180 kcal/gm
γ	=	1.5555
mw	=	31.6
A_r	=	24.0×10^{8} sec^{-1}
E_r	=	3.0×10^{4} kcal
A_τ	=	5.6840×10^{-8} sec^{-1}
E_τ	=	1.5031×10^{4} kcal

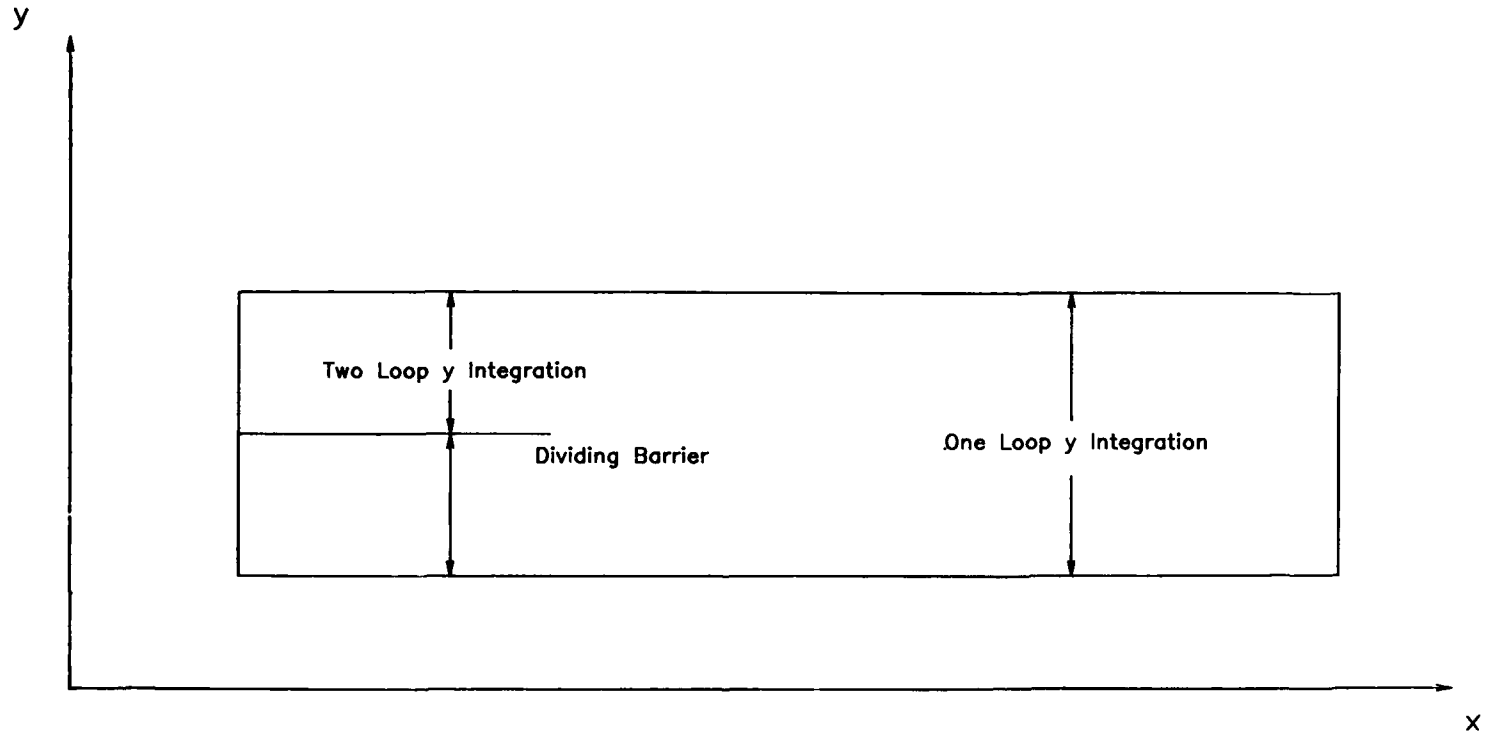

FIGURE 1 Schematic of the Computational Domain

FIGURE 2

Pressure Contour Plots : Non-reactive code.
Initial disturbance on left hand boundary, dividing barrier not yet implemented.

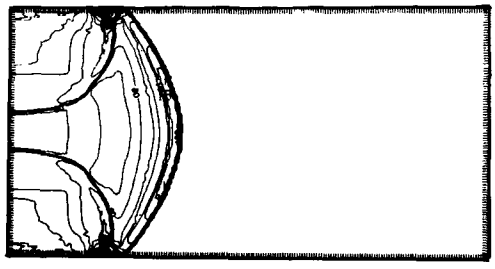

600 cycles

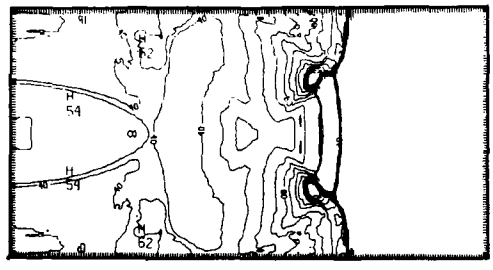

1800 cycles

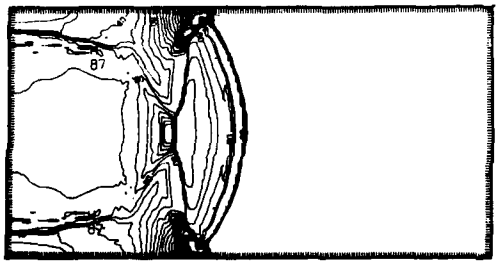

1000 cycles

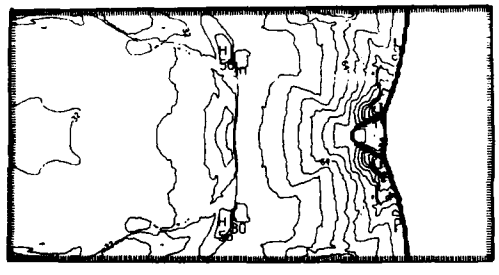

2200 cycles

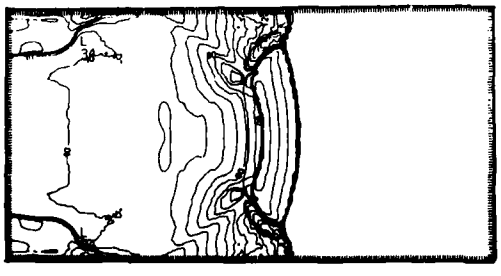

1400 cycles

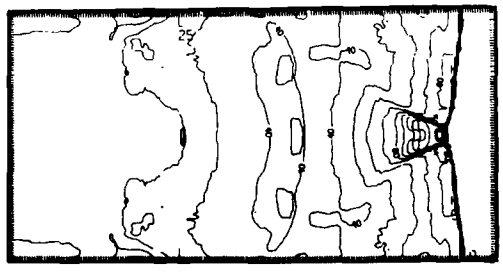

2600 cycles

FIGURE 3

Pressure Contour Plots : Non-reactive code.
Initial disturbance on left hand boundary of upper chamber

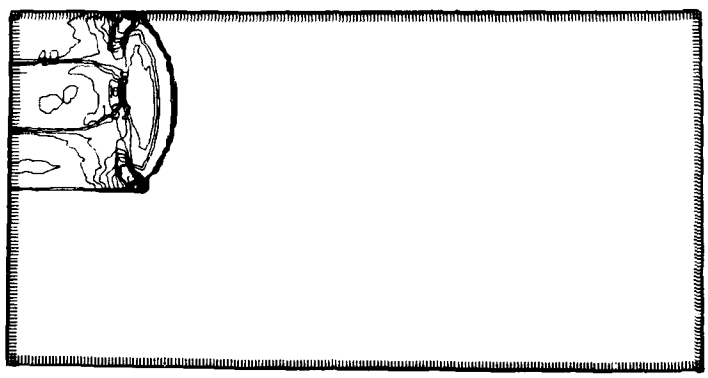

500 cycles

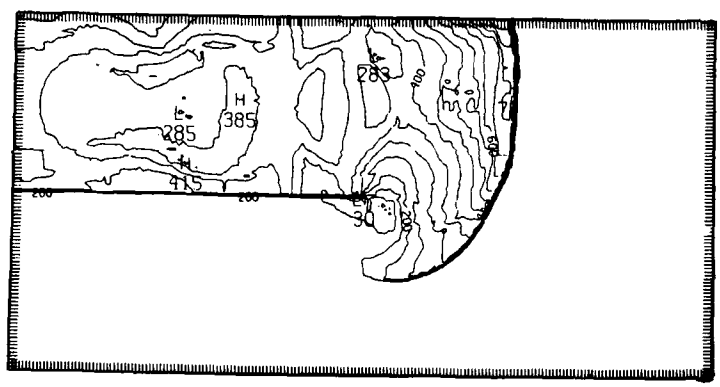

2500 cycles

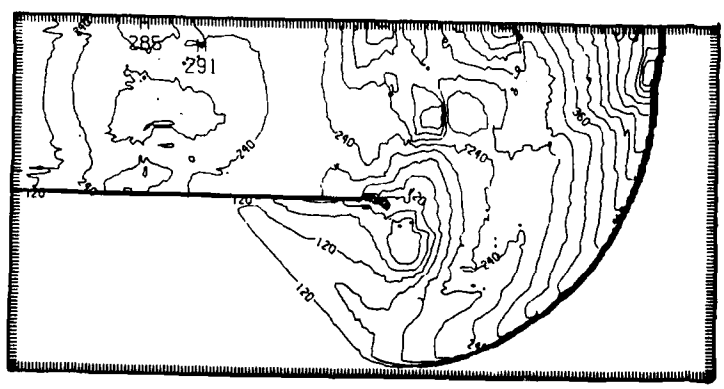

3500 cycles

FIGURE 4

Pressure Contours : Single Species, Reactive
Cycle Numbers 700 to 2800

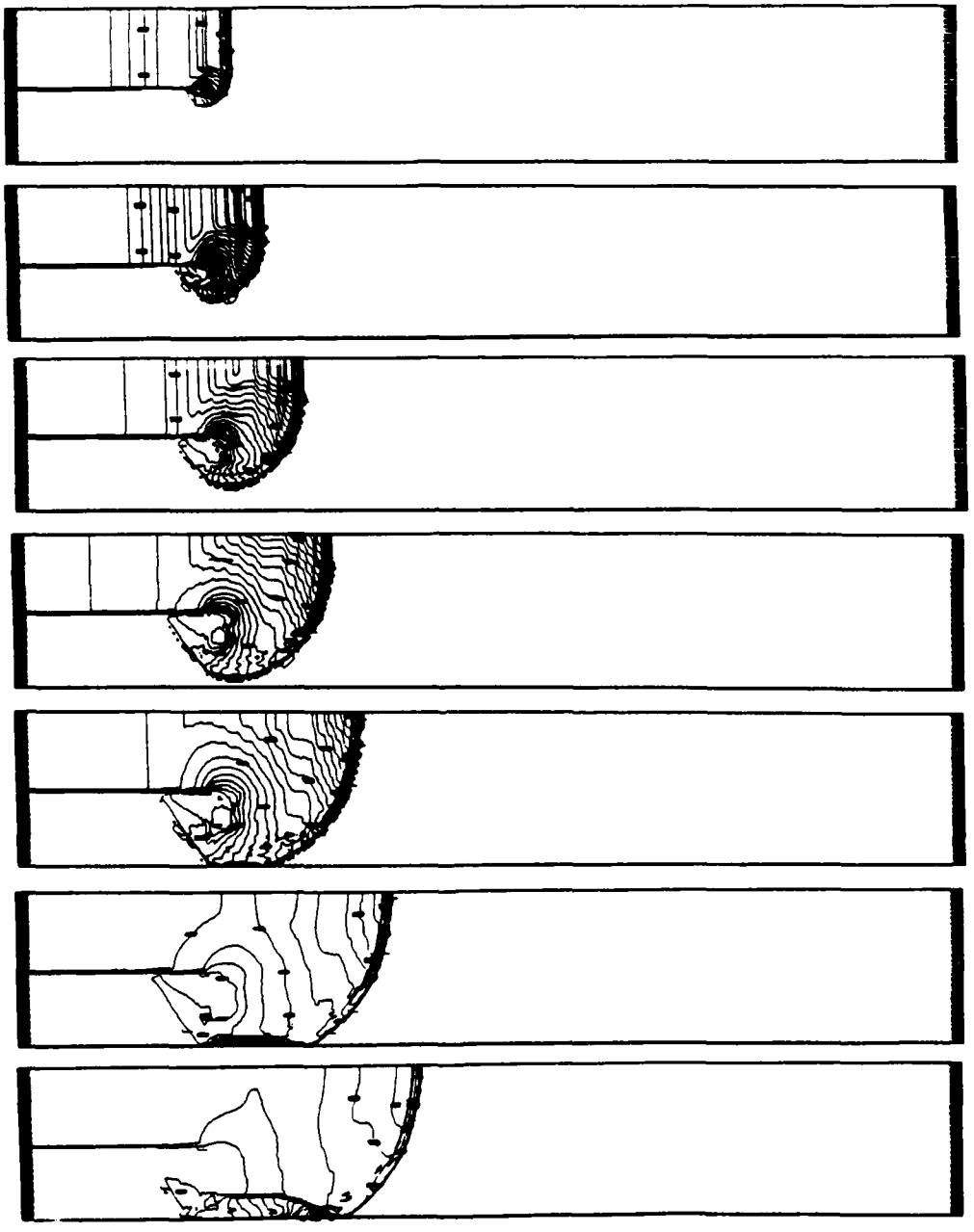

FIGURE 4 continued

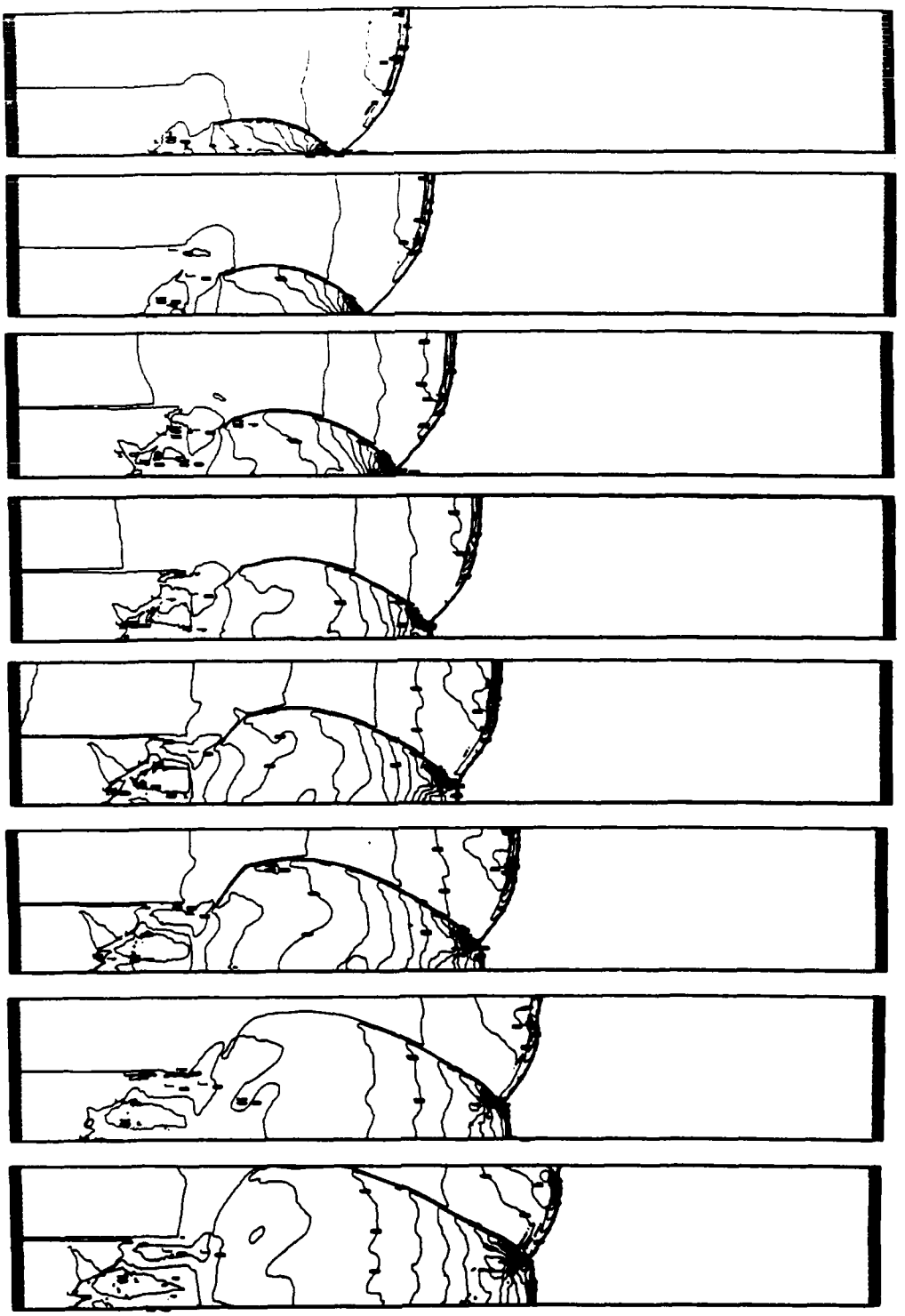

FIGURE 4 continued

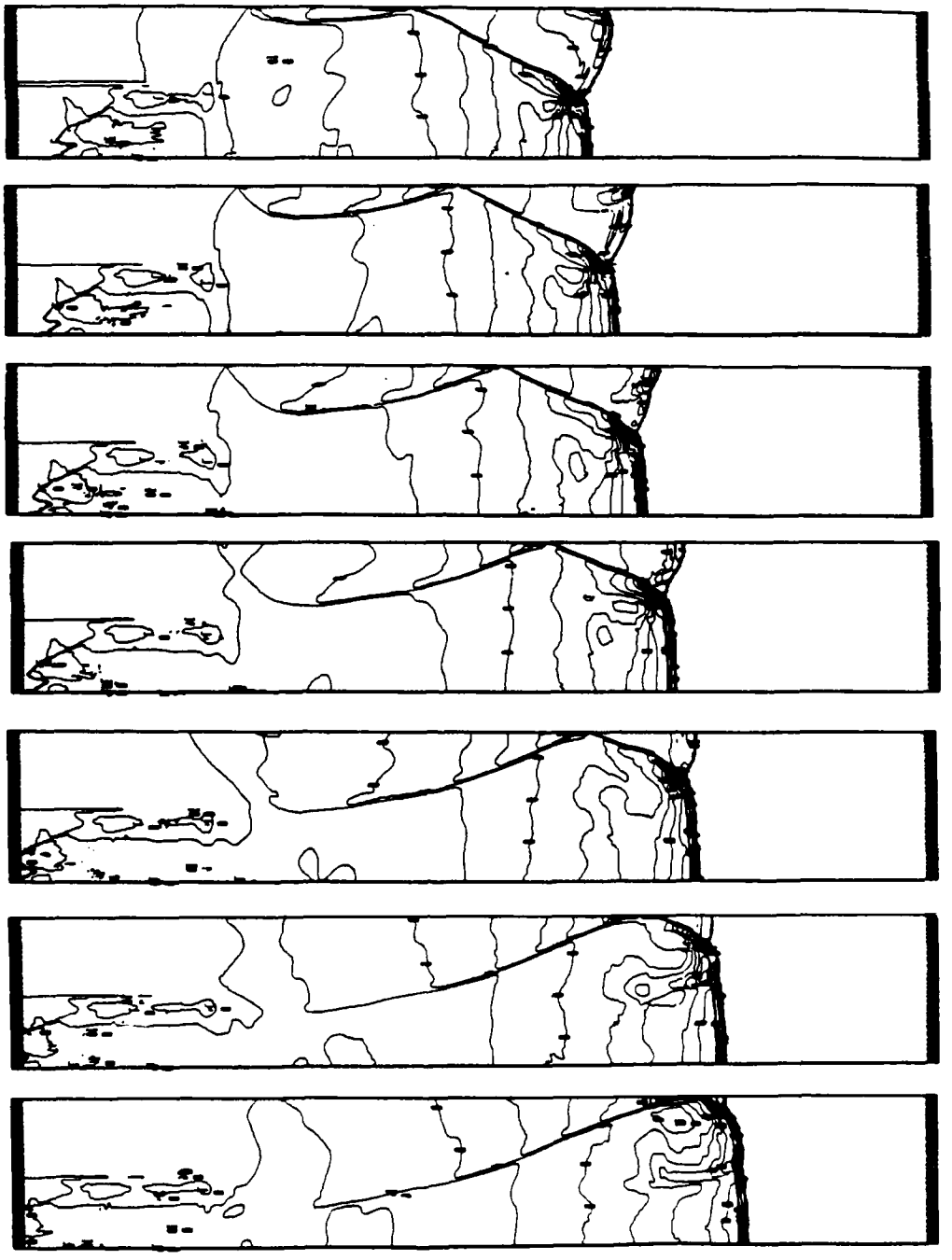

FIGURE 5

Pressure Contours : Two species, one reactive, one inert
Cycle Numbers 700 to 3000

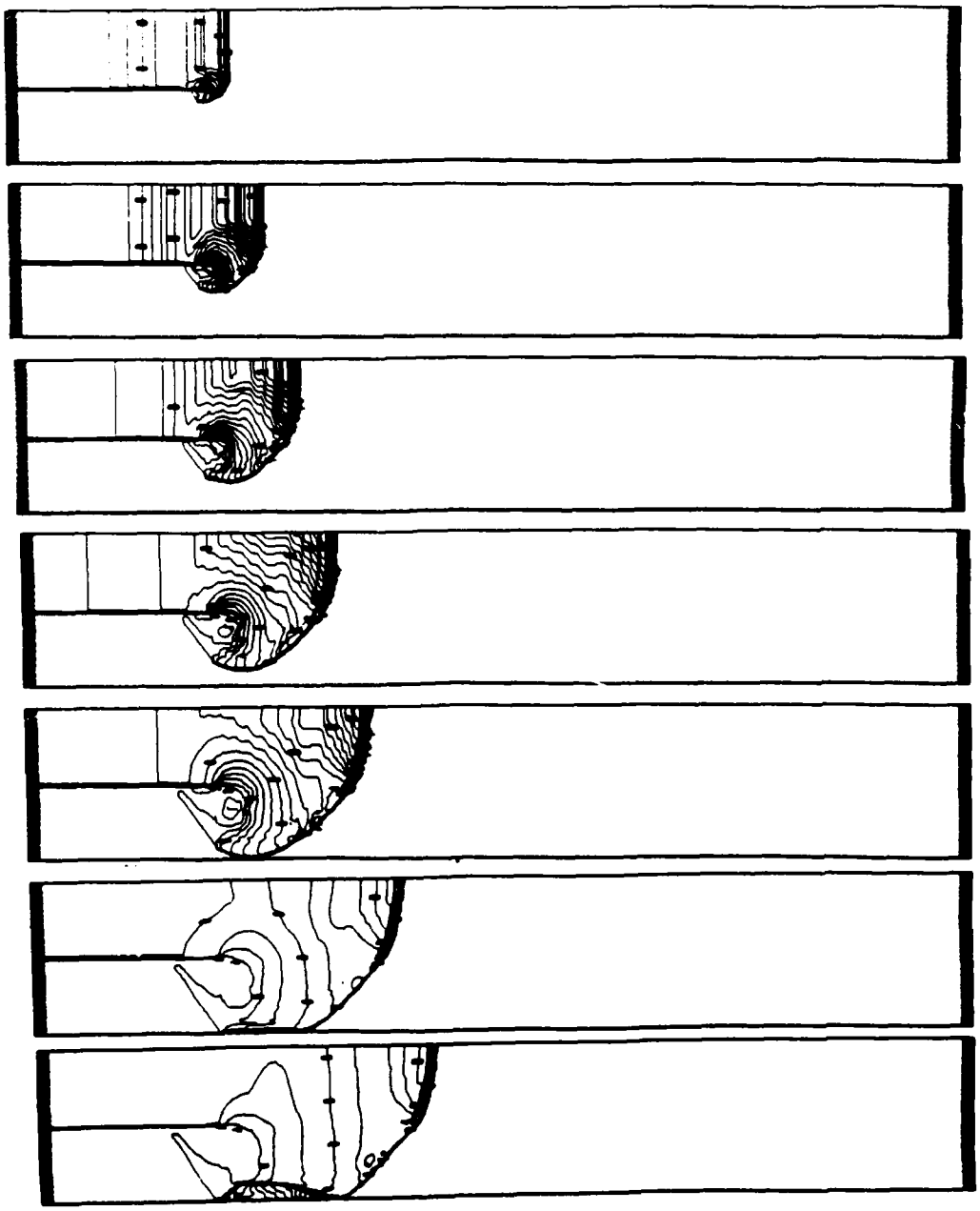

FIGURE 5 continued

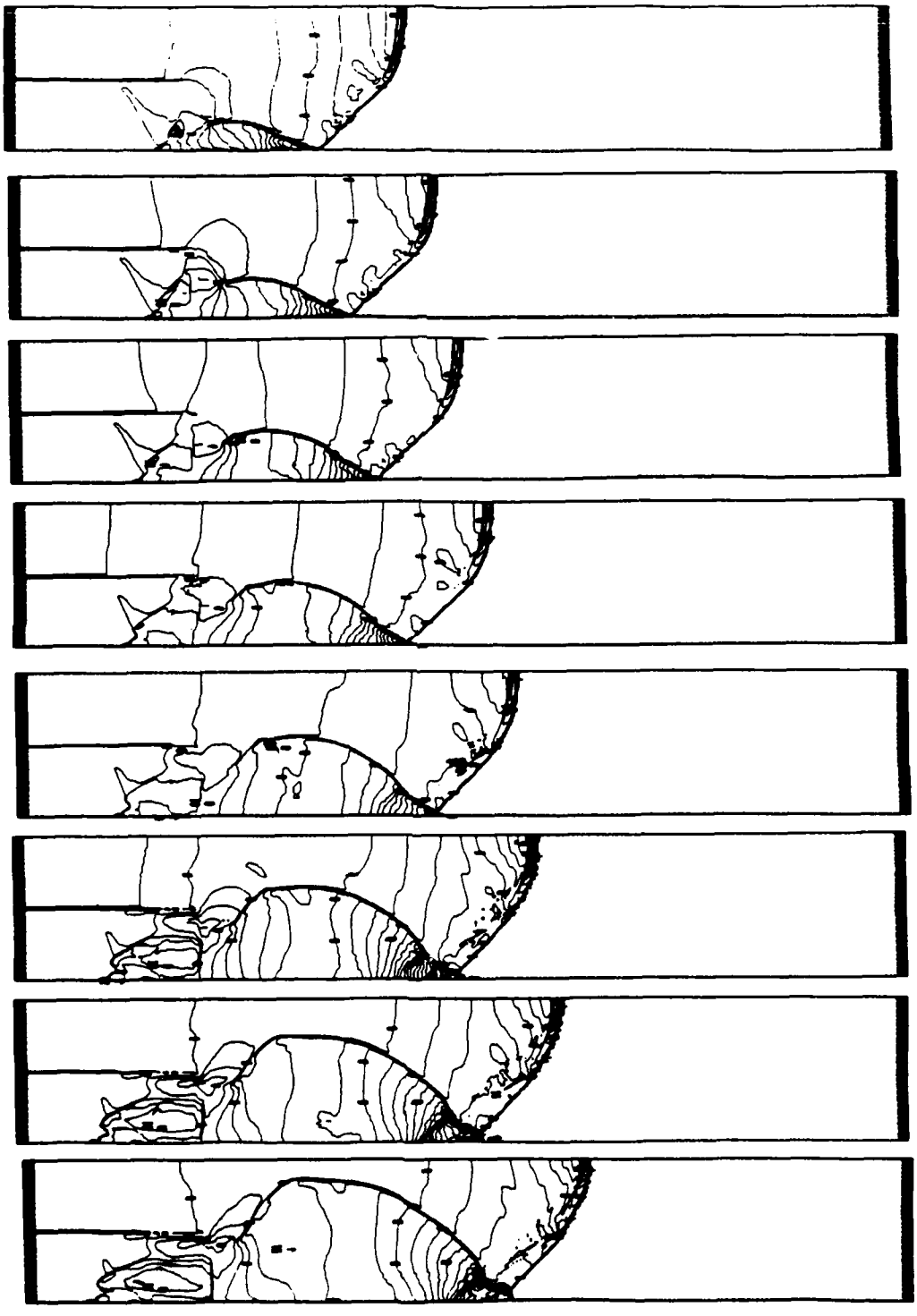

FIGURE 5 continued

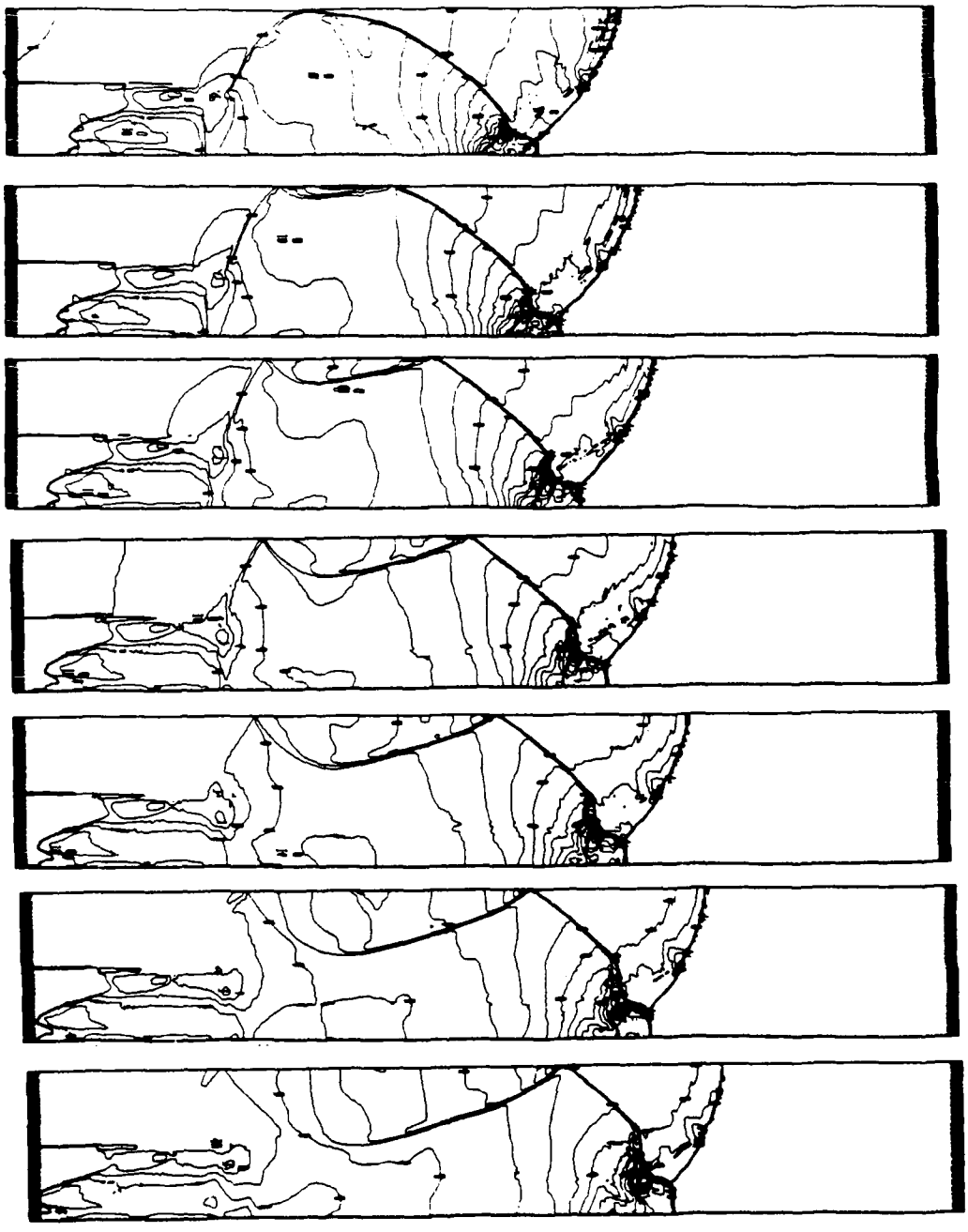

FIGURE 5 continued

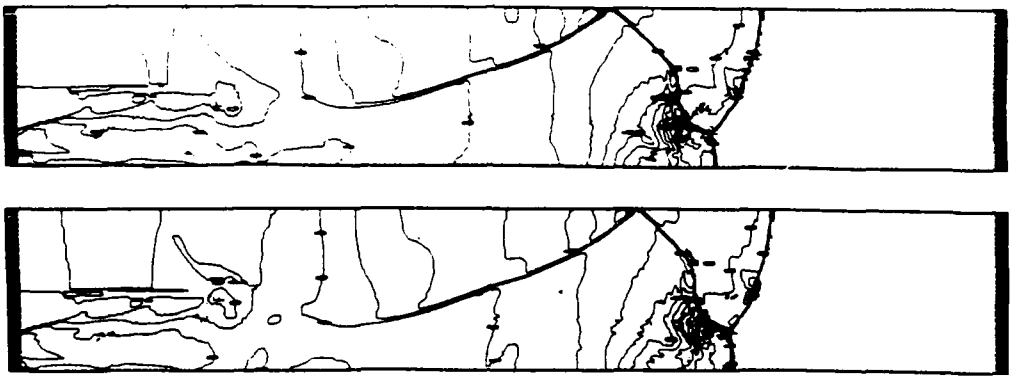

FIGURE 6

Pressure Contours : Two species, with SP1 = SP2
Cycle Numbers 800 to 2000

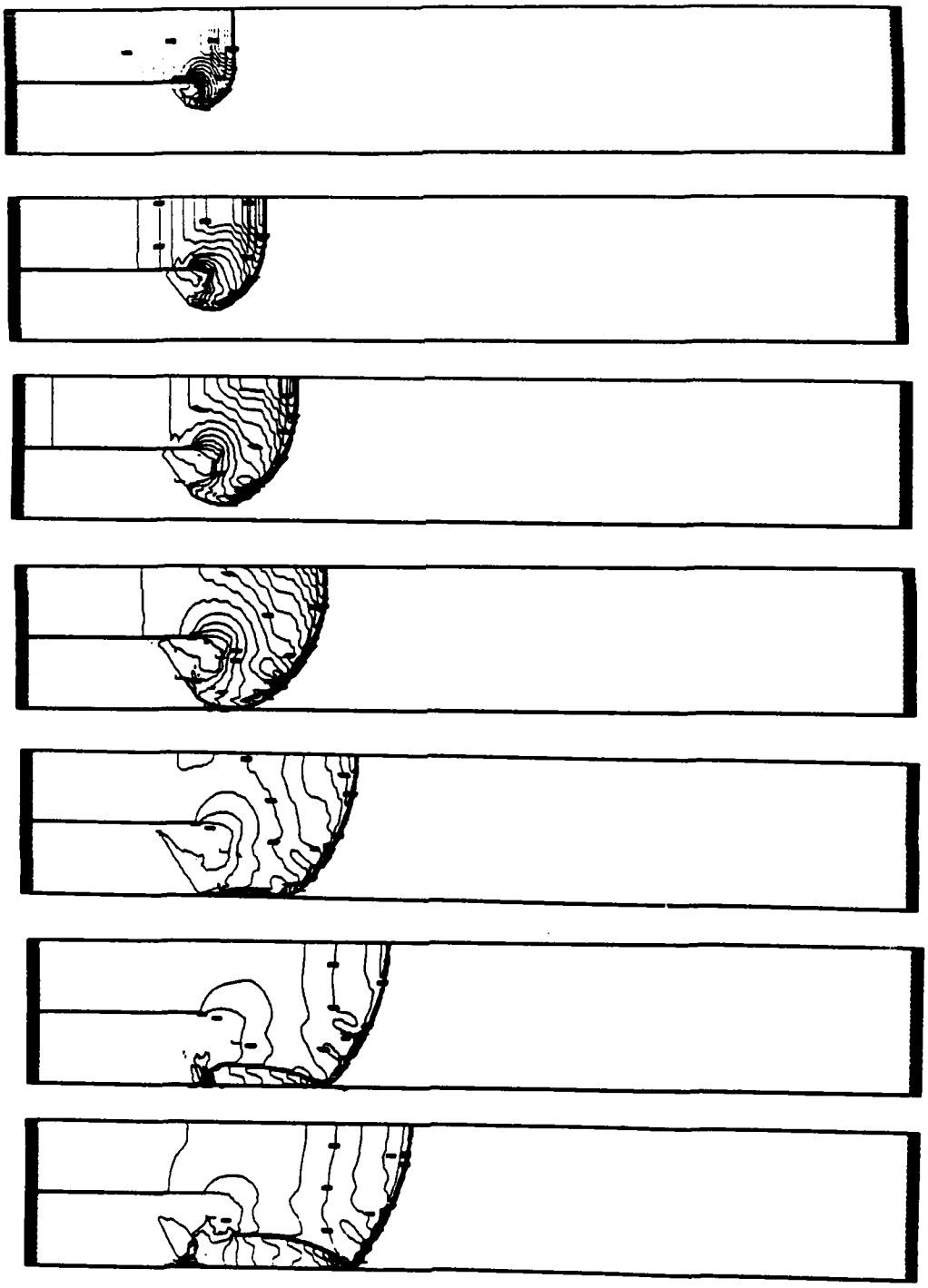

FIGURE 6 continued

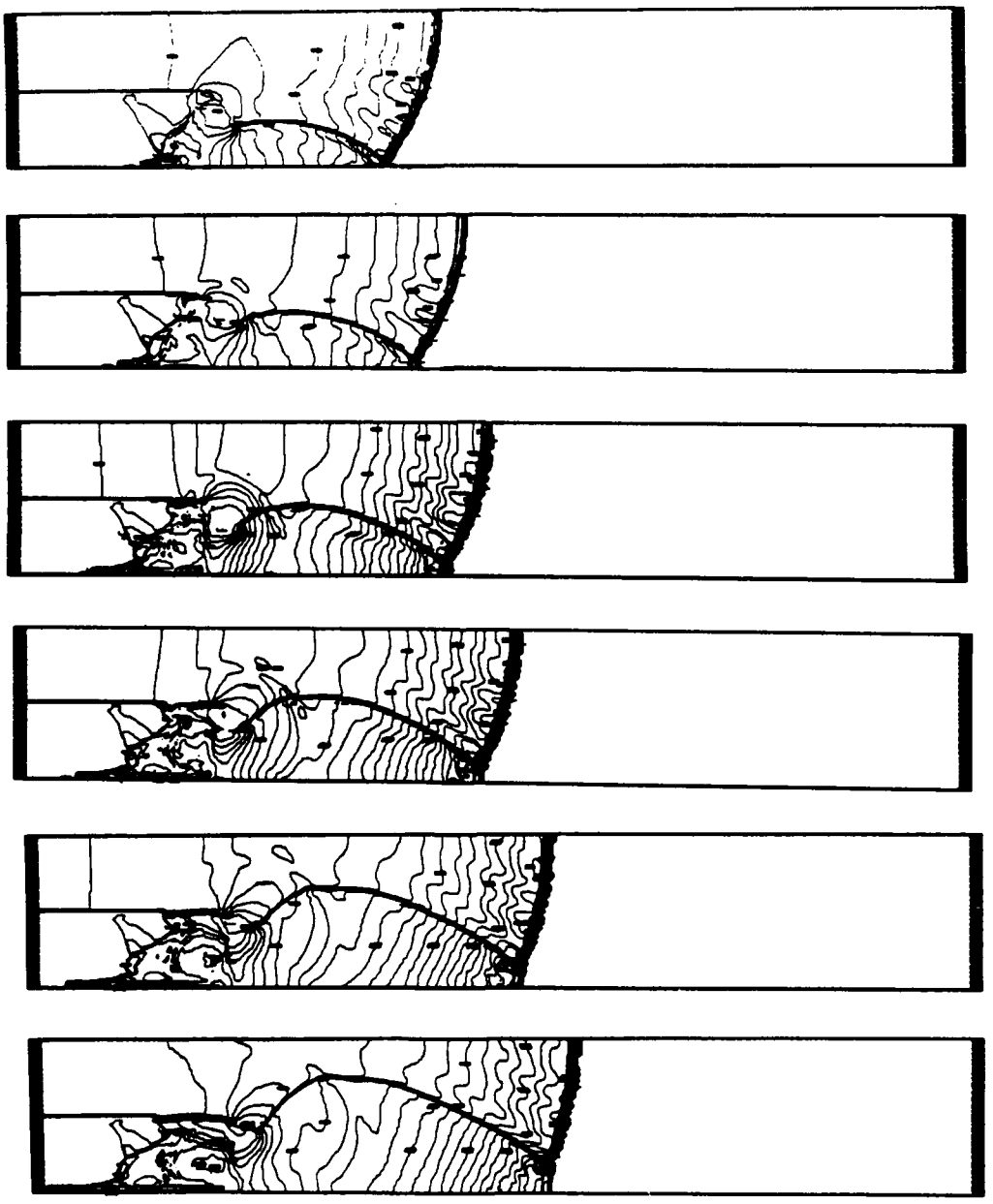

FIGURE 7

Pressure Contours : Two species, $\phi = 0.25$
Cycle Numbers 800 to 2500

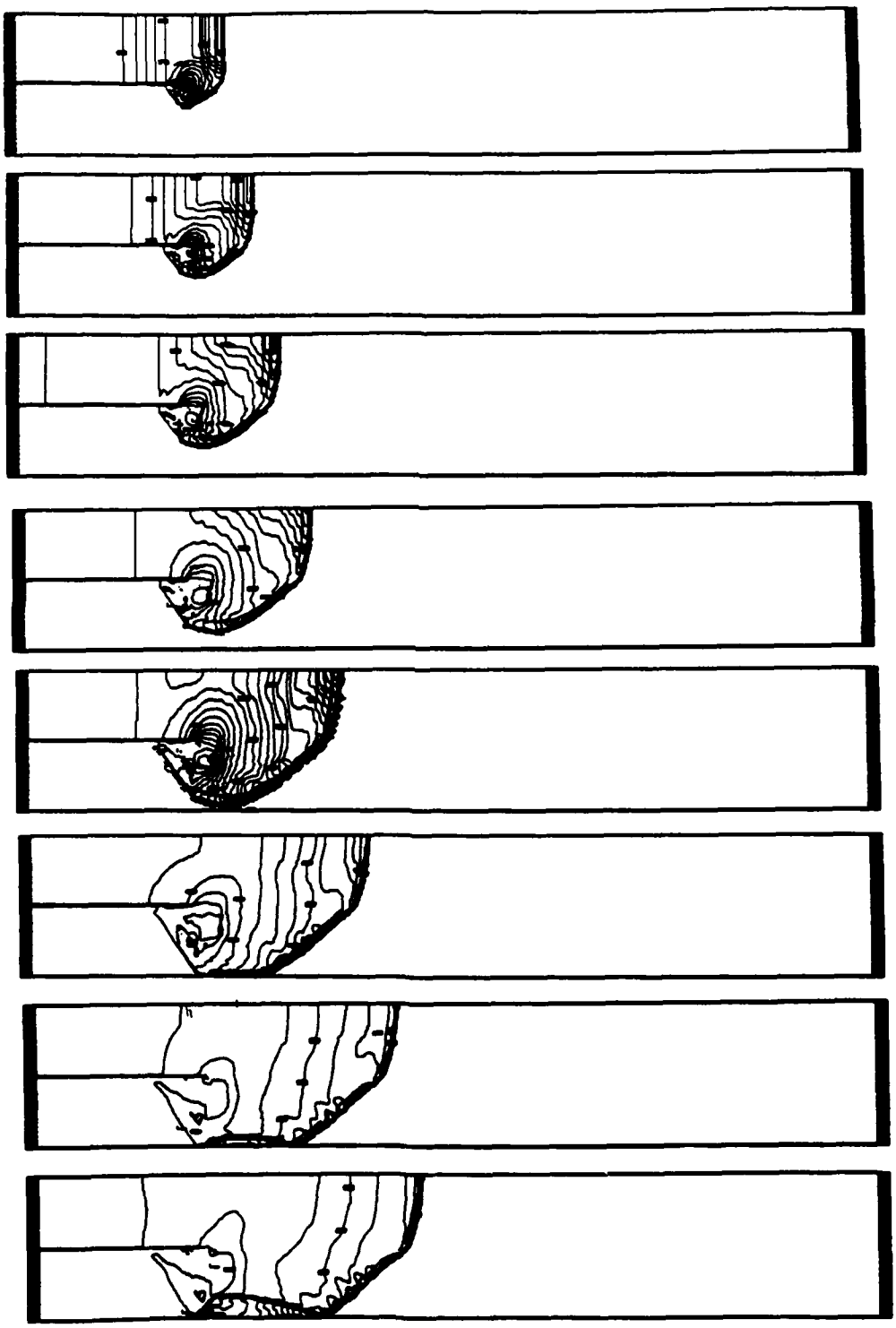

FIGURE 7 continued

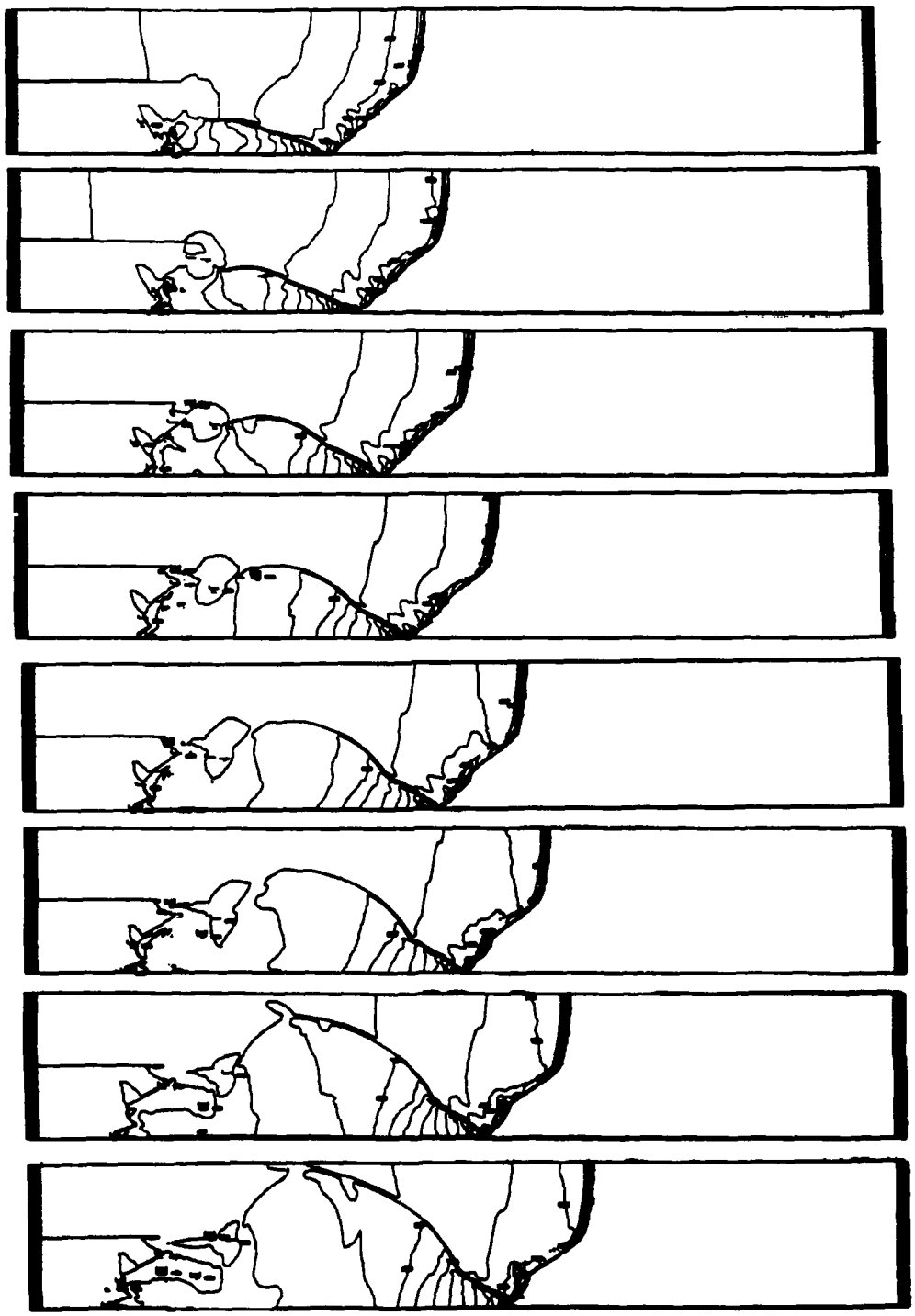

FIGURE 7 continued

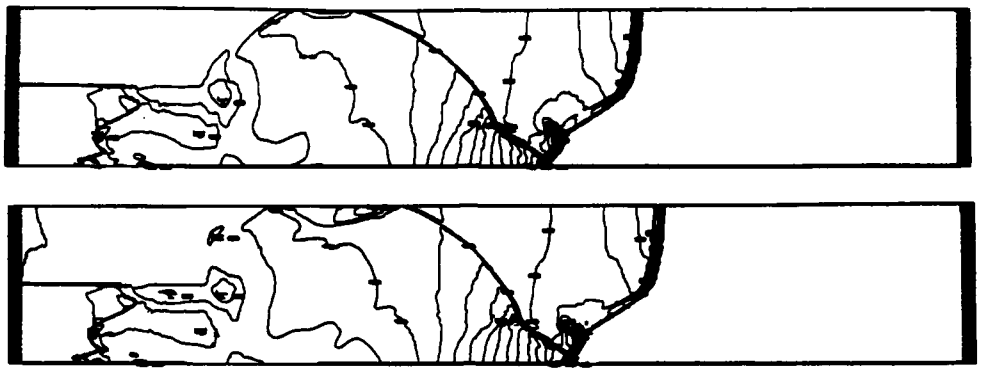

SECURITY CLASSIFICATION OF THIS PAGE **UNCLASSIFIED**

DOCUMENT CONTROL DATA SHEET

REPORT NO.	AR NO.	REPORT SECURITY CLASSIFICATION
MRL-RR-1-89	AR-005-706	Unclassified

TITLE

Numerical simulation of detonation transfer between gaseous explosive layers

AUTHOR(S)

D.A. Jones, R. Guirguis and E.S. Oran

CORPORATE AUTHOR

DSTO Materials Research Laboratory
PO Box 50
Ascot Vale Victoria 3032

REPORT DATE	TASK NO.	SPONSOR
July 1989	DST 88/112	DSTO

FILE NO.	REFERENCES	PAGES
G6/4/8-3732	23	35

CLASSIFICATION/LIMITATION REVIEW DATE

CLASSIFICATION/RELEASE AUTHORITY
Chief, Explosives Division MRL

SECONDARY DISTRIBUTION

Approved for public release

ANNOUNCEMENT

Announcement of this report is unlimited

KEYWORDS

Numerical simulation Simulation Gaseous detonation

SUBJECT GROUPS 0079E

ABSTRACT

The development of a two-dimensional computer code to simulate detonation transfer between explosive layers is described. The code is based on previous models developed at the Laboratory for Computational Physics and Fluid Dynamics at Naval Research Laboratories, Washington, DC to study the structure of layered detonations and the details of detonation transmission from one medium to another. The code has been configured to simulate experiments conducted at the University of Michigan on the lateral transfer of detonation and shock phenomena between different gaseous layers. Preliminary calculations with the code show that the computations produce many of the structures seen in the Michigan experiments and also provide detailed descriptions of the detonation transmission and evolving structure.